A 2D Ray-Tracing Based Model for Micro- and Millimeter-Wave Propagation Through Vegetation

Nuno R. Leonor, Rafael F. S. Caldeirinha, *Member, IEEE*, Telmo R. Fernandes, *Member, IEEE*, David Ferreira, and Manuel García Sánchez, *Member, IEEE*

***Abstract*—A novel two dimensional model to characterize the electromagnetic behavior of trees has been developed with the purpose of being used in ray-tracing based simulation platforms. This model uses various point scatterers with specific radiation characteristics to describe the effect of the trees present in the radiowave propagation path. The method to extract the parameters of the point scatterers from measurements is presented. The performance of this novel formulation is assessed in a tree formation scenario against measurements results obtained in a controlled environment, inside an anechoic chamber, at 20 and 62.4 GHz. Additionally, a comparison analysis with a discretized radiative energy transfer (dRET) approach is conducted, where a relatively good agreement has been found. The absence of readily plug-in models considering propagation through and/or around vegetation makes this new tool interesting for radio planning purposes.**

***Index Terms*—Millimeter wave radio propagation, modeling, ray tracing, scattering, vegetation.**

I. Introduction

The phenomena inherent to radiowave propagation through vegetation areas have raised particular interest among researchers in the past decade [1]. In the particular case of terrestrial mobile networks, vegetation may influence the propagation of radiowaves, causing its attenuation, scattering and/or depolarization [2]. Noteworthy, the irregular shapes, the inhomogeneous and the time variant properties of trees yield to one of the most complex topics of research in radiowave propagation [3].

Empirical [4]–[7] and semi-empirical [8], [9] models, relying on simple exponential equations, have been successfully used to describe the signal attenuation and the well known "dual-slope" effect observed along the radio path inside a vegetation medium [8]. Nevertheless, due to their scenario-specific nature, e.g., frequency, scenario, species, etc., the accuracy of such models becomes questionable in scenarios outside the model scope [10].

Manuscript received May 02, 2014; revised September 29, 2014; accepted October 01, 2014. Date of publication October 08, 2014; date of current version November 25, 2014.

N. R. Leonor and D. Ferreira are with the Instituto de Telecomunicações, Leiria, Portugal and also with the University of Vigo, Dept. Teoria do Sinal e Communicacins, Vigo, Spain.

R. F. S. Caldeirinha and T. R. Fernandes are with the Instituto de Telecomunicações-Leiria, Portugal, with the Polytechnic Institute of Leiria, School of Technology and Management, Portugal, and are also with the University of South Wales, Wireless and Optoelectronic Research and Innovation Centre, Pontypridd, U.K. (e-mail: rafael.caldeirinha@ipleiria.pt).

M. G. Sánchez is with the Universidade de Vigo, Dept. Teoria do Sinal e Communicacins, Vigo, Spain.

Digital Object Identifier 10.1109/TAP.2014.2362124

On the other hand, theoretical models relying on mathematical formulations are suitable for site-specific scenarios, effectively characterizing each physical phenomena involved in the propagation of radiowaves. These models are often very complex in nature, requiring numerical approximations to provide accurate solutions. The modeling of the propagation of radiowaves through tree foliage with theoretical models, generally requires accurate electromagnetic description of the tree geometry, including branches and leaves.

Two different types of theoretical models are presented in the literature. One method is based on the consideration that the vegetation medium is homogeneous and should be treated as an isotropic dielectric material with constant permittivity and conductivity [11]–[13]. However, this is not always the case, since vegetation, in general, is inhomogeneous and space gaps may exist between adjacent trees.

In the second, the volume is considered to be heterogeneous, where vegetation is described as a mixture of trunks, branches, leaves and air, represented by randomly distributed thin lossy dielectric disks and finite lossy dielectric cylinders, as in [14]–[16]. Alternatively, the volume can be generated yielding a realistic fractal engine based on Lindenmayer systems [17], as in [18], [19]. In both approaches, wave theory is used to evaluate the total scattered field, using Foldy's approximation [20]. These models were successfully used providing relatively good predictions of total scattered field. However, their integration with commercial simulation platforms (e.g. ray-tracing) may become prohibitive due to their mathematical complexity, and extraction difficulty of the required input parameters, e.g., leaf density, area and thickness, in a real-sized forest [21].

The radiative energy transfer (RET) [22] model is another type of theoretical approach. Indeed RET based models have successfully been used to simulate radiowave propagation in vegetation environments, as presented in [23]–[25]. Such studies were conducted, namely: in the vegetation cells input parameter extraction of various species at various frequencies; on the performance analysis of the referred model while predicting the received signal inside and around a tree formation; and on the feasibility of introducing time variant input parameters to consider the wind-induced dynamics. Hitherto, RET theory [22], in general, and discrete RET [26], in particular, have been used to model the propagation phenomena in random scattering media, presenting a relatively good performance when compared to measurement results. However, the difficulty arises when extracting the input parameters of RET based models, in addition to the implementation complexity and with the fact that dRET model requires discretization of the vegetation volume into small cells. And thus, it is numerically intractable for large propagation distances [10], and subsequently it may preclude its integration with existing commercial simulation platforms and other simulation algorithms.

However, the applicability of geometrical/uniform theory of diffraction (GTD/UTD) based models to predict the behavior of radiowave propagation in vegetation volumes seems to be limited to frequencies below 3 GHz [3]. This is due to the complex nature of the vegetation medium which is not compatible with the deterministic approach of the GTD/UTD theory. This becomes more critical at higher frequencies, in which the size of leaves and smaller branches presented in the canopy becomes comparable to the propagating signal wavelength.

Ray-tracing based methods have also been proposed in [27], [28] to evaluate vegetation attenuation and scattering. The first presents a propagation model for urban environments, which is based on uniform theory (UTD) multiple diffraction. This model takes into account the propagation over buildings, and to some extent, the excess loss introduced by vegetation. The later is based on a fractal tree generator to develop a physical model of the trees present in the radio path, and uses geometric optics to evaluate the total scattered field caused by vegetation elements. However, due to the complex nature of the vegetation medium and the deterministic approach of the GTD/UTD theory, modeling the propagation phenomena in a real-sized forest, might become prohibitive, since physical parameters, such as, size, position, and orientation angle of the trees present in the radio path have to be taken into account. This becomes more critical at higher frequencies, in which the size of leaves and smaller branches presented in the canopy becomes comparable to the propagating signal wavelength.

To overcome these limitations, a feasibility study on vegetation modeling using scattering points distributed in a computational volume, is presented. Following the encouraging initial results presented in this paper, further work needs to be undertaken in this area in an effort of developing a generic doubly-selective 3D ray-tracing based model applied to canopy, trunk and ground layers. And thus, one needs to effectively characterize the radiowave (spatio-temporal) propagation phenomena through vegetation media, including attenuation (absorption), (diffuse) scattering, depolarization and time-variability.

This paper is then organized as follows. In Section II, an overview of the model rationale and development, namely the ray-tracing algorithm adopted to gather the interactions between 2 or more obstacles, as well as the method used to evaluate the total received signal, is presented. In Section III, a brief overview of the measurement systems used throughout this paper is presented. Section IV addresses a feasibility study of extending the point scatterer formulation to characterize the re-radiation pattern of a single tree. For that purpose, a 2D physical model to represent the tree volume is presented, as well as its input parameters. It is also presented, in this section, a detailed description of the method used to effectively extract the proposed model parameters, and root-mean square error (RMSE) analysis of the proposed model, against measurements results obtained in a controlled environment, for several trees at two different frequencies. Section V presents the performance analysis of the proposed model extended to tree formations scenarios, not only against the dRET modeling approach [23], but also, against measurements performed in an anechoic chamber. Finally Section VI draws conclusions and points out directions for further work.

II. Simulation Platform Overview

A. Ray Tracing Algorithm

It is reasonable to state that ray-tracing based simulation platforms are divided into two major groups, i.e., those using method-of-images formulations [29] and ray-launching algorithms [30].

The former determines the multipath sources using image theory, up to a specified order. That is, the algorithm might include all first-order, second-order, and up to the Nth order reflection paths. Since image theory determines exact radiation paths, the method of images introduces no errors into the radiation paths. However, this method is solely valid for reflected modes of propagation, since diffraction introduces infinite degrees of freedom in the direction of a ray path [30]. On the other hand, in ray-launching algorithms, the propagating rays are homogeneously launched from a unit sphere centered at the transmitter location, and all regions are evenly covered by rays. Rays that intersect a detection area (reception sphere) around the receiver, after a number of reflections, transmissions, and diffractions, will be accounted for the received signal. Since the computational effort increases with the increase in angular resolution, often this algorithm is needed to calculate multipath components that will not intersect the reception sphere, leading to be an inefficient method for large simulation scenarios.

Therefore, among the ray-launching techniques there are some variants that take into consideration the geometric obstacles present in the simulation channel using groups of point scatterers. These points are characterized by a particular re-radiation function, depending on the obstacle characteristics, which affects the relationship between incident and scattered rays, both in amplitude and phase. Subsequently, an intelligent ray-tracing algorithm is used to gather all the interactions between the obstacles present in the computational volume, where only relevant propagation paths are considered [31]–[33]. This ray-tracing method also supports multiple order simulations, that is, the number of interactions between different scatterers, which can be defined while implementing the algorithm. For the purpose of this paper, a second order ray-tracing algorithm was adopted, as in [31].

In the first iteration, this algorithm calculates both the direct ray, and also the rays traveling from the transmitter to the receiver antenna, for all the point scatterers defined in the geometry. However, when considering propagation phenomena such as double diffraction or interactions between two (or more) distinct obstacles, a second simulation step was introduced. In the latter, point scatterers are considered to be illuminated by rays generated in the first iteration, and thus, acting as new transmitters. To this extent, rays from the first scatterer to all other point scatterers are defined in the simulation geometry and are reflected (or diffracted) to the receiver. Rays from both first and second iterations are depicted in Fig. 1. Therefore, a simulation using this algorithm, exhibits a number of multipath components defined by $(N_{\text{paths}} = N_{\text{scatterers}}^2 + 1)$.

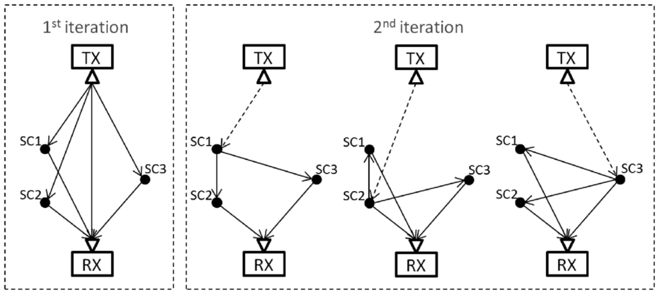

Fig. 1. Iterations of ray-launching algorithm.

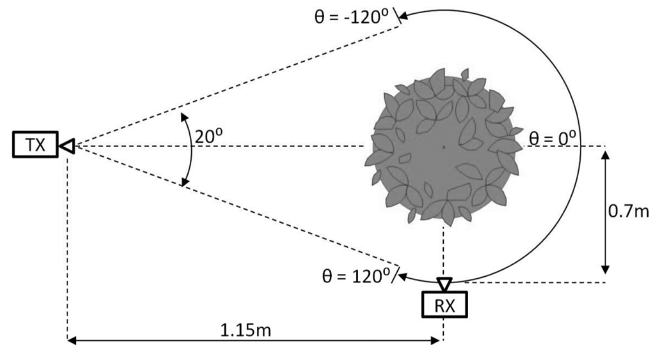

Fig. 2. Tree re-radiation measurements geometry.

B. Simulation Results

The received signal complex envelope is calculated by adding all the multipath components arriving at the receiving antenna, for each step of the mobile movement and/or point scatterers, using (1), where N_{paths} is the number of multipath components arriving at the receiver, d_i is the distance traveled by the ith component and a_i represents the attenuation caused by the channel to that particular component

$$\mathrm{Signal}_{\mathrm{complex}_{\mathrm{env}}} = \sum_{i=1}^{N_{\mathrm{paths}}} \frac{e^{\left(\frac{-i2\pi d_i}{\lambda}\right)}}{\left(\frac{4\pi d_i}{\lambda}\right)^2} \times \frac{1}{a_i}. \quad (1)$$

Furthermore, when considering the effects of both transmitter and receiver antenna radiation patterns, the received signal components must be convolved with the corresponding antenna radiation patterns, considering the antenna orientation angles and the angles of arrival and/or departure of each multipath component. It is also important to highlight that, due to the iterative nature of the proposed simulator, the channel was considered stationary during each time step, i.e., wide sense stationary uncorrelated scattering (WSSUS) channel.

III. Measurement System Overview

A. 20 GHz Measurement System

The 20 GHz measurement system is comprised of a Gunn diode voltage controlled oscillator, providing a continuous-wave (CW) tone at 20 GHz, which is radiated to the radio path by a 17° beamwidth 20 dBi standard horn antenna. The receiver employed a similar 20 dBi horn antenna coupled to a frequency mixer for down conversion of the received signal to an IF of 220 MHz, which was amplified by a 44 dB low-noise amplifier, and acquired by a spectrum analyzer (SA) remotely controlled by a GPIB interface. To protect this measurement system, attenuators were included in both transmitter and receiver for proper adjustment of the signal levels, providing an overall system dynamic range of about 175 dB.

B. 62.4 GHz Measurement System

In the 62.4 GHz measurement system, a phase-locked oscillator was used to generate a CW of 62.4 GHz, which was radiated by a 25 dBi standard horn antenna. This signal was then received by a similar antenna to that of the receiver, down-converted to an IF of 600 MHz, by a mixer with a LO of 61.8 GHz, and acquired by a SA. Similarly to the 20 GHz measurement system, attenuators were used to extend the overall dynamic range of the measurement system up to about 180 dB, without damaging any system component.

IV. Extension of Point Scatterer Formulation to Single Trees

In this section, a feasibility study of extending the point scatterer formulation presented in [31] to characterize the re-radiation pattern of a single tree, is presented. This study was based on specific measurements using 13 *ficus benjamina* and 16 in-leaf conifer trees, providing a sparse and dense foliage structure, respectively, at 20 and 62.4 GHz.

A. Methodology and Measurement Geometry

In order to understand the effects caused by an isolated tree on the propagation of radiowaves, appropriate re-radiation pattern measurements were conducted on two different tree species, for both frequencies.

The measurement geometry depicted in Fig. 2 was set in a controlled environment, inside an anechoic chamber, to minimize interferences from unwanted reflections. The transmitter was placed at a distance of 1.15 meters from the tree under measurement, which is enough to ensure that the tree was illuminated by a plane wave. The receiver was maintained at a constant distance of 0.7 meters, and rotated along an arc around the tree, within an angular range of $\theta = -120°$ to $\theta = 120°$, with increments of 1°. This rotation was performed by an automated mechanical rig fully controlled by a software application, therefore minimizing human errors. During these measurements, both transmitter and receiver were set at a height of 1.4 meters above the ground.

Fig. 3 shows the re-radiation measurement results for both *ficus benjamina* and conifer trees under study obtained at 20 and 62.4 GHz. Based on these measurement results, it is clear that the tree will not only cause insertion loss in the forward (main) lobe, but it also contributes to an increased signal level in the backscattering region, due to the tree scattering, confirming previous findings [23]–[25]. In the particular case of the conifer tree, due to its greater foliage density, the insertion loss is observed to be higher than the *ficus* tree, representing a significant reduction of the forward lobe to a level close to the backscattering region.

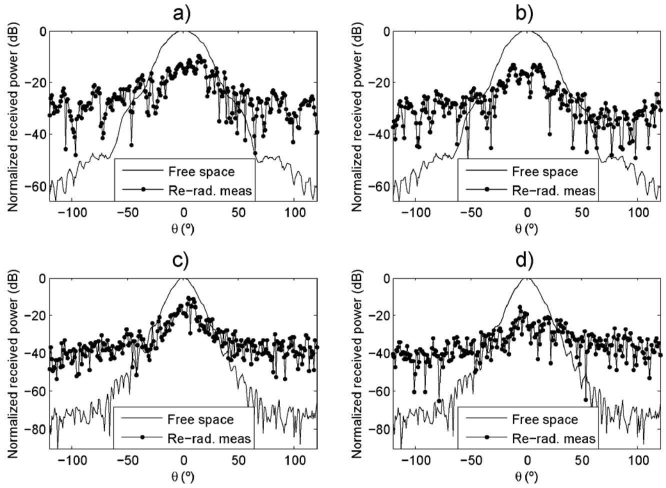

Fig. 3. Re-radiation pattern examples: a) *ficus benjamina* and b) coniferous, at 20 GHz; c) *ficus benjamina* and d) coniferous, at 62.4 GHz.

B. Modeling Trees Using Point Scatterers

Following a detailed characterization of the tree re-radiation patterns, several studies were performed to assess the feasibility of modeling the canopy phenomena based on ray-tracing theory using point scatterers. Results have clearly indicated the potential of using such approach, opening several research avenues, e.g., make use of the statistical distribution of point scatterers (in a cluster) to induce time-varying signal effects due to wind. However, for the purpose of this paper, only the 2D static modeling approach is described.

1) Excess Attenuation: For the purpose of extending the proposed formulation to isolated trees, it was first necessary to assess whether or not a tree shape can be mapped onto an area in the simulation space. Considering the various size and the usual cone like shape that trees may exhibit in nature, for the 2D modeling approach, a cylindrical shape with varying radius was defined to represent a tree canopy.

Additionally, propagation rays traveling through a vegetation area, may suffer an additional attenuation, other than free space loss, due to leaf absorption and scattering [1]. However, the method to evaluate the amount of excess loss presented in [1], is rather complex and its input parameters are difficult to extract. Therefore, the development of a simpler propagation model to evaluate the excess path loss of signals propagating through a vegetation area, was developed.

The proposed additional excess loss model is given in (2), where d is the distance traveled by each ray inside the vegetation media and Att_k is an input parameter that will be adjusted depending on the propagation characteristics of the specific tree

$$L_{Ex} = d \times Att_k + 1. \tag{2}$$

2) Point Scatterers re-Radiation Function: The definition of the re-radiation pattern of the point scatterers mimicking the trees is an important issue addressed in the proposed model. Results of an initial study based on RMSE analysis between simulated and measured re-radiation patterns, suggest that no significant correlation exists between the re-radiation function of each individual point scatterer and the overall re-radiation pattern. In fact, this imposes to a certain extent some degree of freedom that can be applied in the new modeling approach. And thus, the error associated to the chosen individual radiation pattern can be easily corrected by adjusting other input parameters, such as, the excess loss applied to each ray traveling through the tree cross section, and the number and distribution of the point scatterers. However, as previously found by the authors in [23]–[25], the signal re-radiation pattern of a tree, which is angular dependent, can be represented by a Gaussian shaped forward (main) lobe, superimposed to an isotropic level, representing the backscattering region, mainly due to diffuse scattering from leaves, twigs and branches.

To this extent, in order to model the re-radiation function of the point scatterers, the empirical model originally presented in [34], and widely used in subsequent researches, which is known as phase function, was employed. In [34], it was concluded that co-polarized scattering patterns (i.e. VV or HH), were similar. The same was observed for cross-polarized patterns (i.e. VH or HV). This phenomena was latter confirmed in [2], where it was concluded that the scattered components are severely depolarized. In this paper only the co-polar component was considered.

The excess loss caused by the trees was evaluated by (2), therefore the propagation model presented in [34], was adapted to be normalized. The final empirical model applied to the point scatterers is presented in (3), where γ is the angular difference (in radians), between the incident and scattered rays, while α controls the level of the scattered power and β is the forward lobe beamwidth. These input parameters, representing the scattering behavior of the vegetation must be extracted according to the method presented in Section V

$$\rho(\gamma) = \frac{\alpha\left(\frac{2}{\beta}\right)^2 e^{-\left(\frac{\gamma}{\beta}\right)^2} + (1-\alpha)}{\alpha\left(\frac{2}{\beta}\right)^2 + (1-\alpha)}. \tag{3}$$

One should note that the propagation model presented in [34] is an approximation, therefore several parameters, such as dielectric constant of leaves and branches, incident polar angle in reference of the angular distribution of leaves and branches, and scatter polar angle in reference of the angular distribution of leaves and branches, are not taken into account.

3) Number of Point Scatterers and Its Distribution: Modeling tree canopies using point scatterers leads to several configurations of number of points and their spatial distribution. Hence, a trade off between these, the computation complexity and accuracy of the predicted results, must be achieved. To this extent, a parametric study based on the influence of above mentioned input parameters, was conducted.

Several simulation were performed contributing to a thorough understanding of the influence of each input parameter in the predicted re-radiation function. One of the most relevant results of this analysis is depicted in Fig. 4. In this study, one may observe, not only the influence of the number of point scatterers defined in the vegetation volume, but also the influence of their distribution. For such analysis, a simulation geometry similar to the one depicted in Fig. 2 was adopted, and the input parameters α, β and Att_k were kept constant and equal to 0.5, 20° and 10 dB, respectively. The point scatterers were randomly distributed

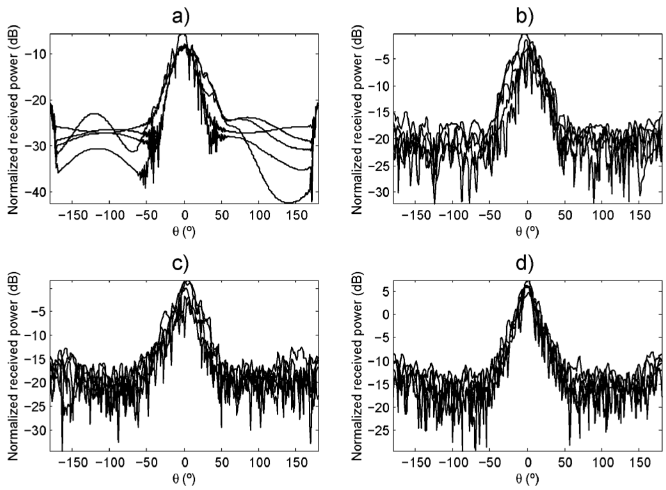

Fig. 4. Several re-radiation pattern simulations for # point dependence analysis: a) 1, b) 5, c) 10 and d) 20 point scatterers.

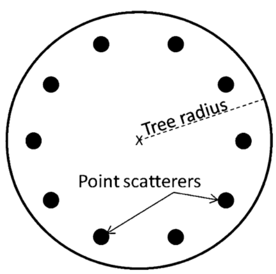

Fig. 5. Scattering point distribution for a single tree.

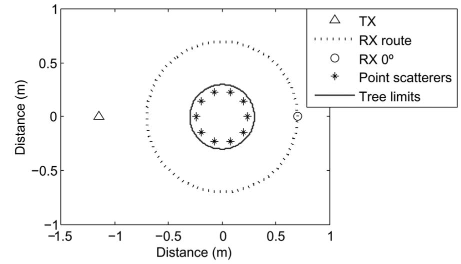

Fig. 6. Simulation geometry adopted for trees' input parameters extraction.

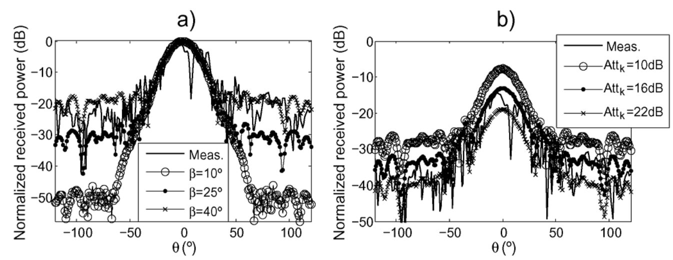

Fig. 7. Examples of input parameters evaluation: a) β; b) Att_k.

inside the tree volume. Fig. 4 presents some samples of the obtained results for 1, 5, 10 and 20 point scatterers randomly distributed, a, b, c and d, respectively.

From the findings in [23]–[25], re-radiations pattern of trees exhibit a Gaussian-like function with an isotropic level in the backscattering region. By observing the results depicted in Fig. 4, one may conclude that, as more point scatterers are defined in the vegetation volume, more Gaussian-like and regular is the re-radiation pattern. Nevertheless, by increasing the number of points linearly, the number of multipath components will increase exponentially. Therefore, a tradeoff between accuracy and computational effort must be achieved. For the purpose of the proof-of-concept presented herein, a tree was defined using 10 point scatterers. As far as the point distribution is concerned, one may also observe in Fig. 4 that for a certain number of point scatterers (e.g. 10), different distributions will yield to slight different re-radiation patterns. This leads one to conclude that different point distributions may be used to characterize the same tree, since other input parameters are adjusted conveniently.

Therefore, with the purpose of reducing the model parameters, the distribution of the point scatterers was set to be constant, using 10 points uniformly distributed in a circle with a radius that is 80% of the real tree radius. Fig. 5 depicts the tree physical model, where the circle represents the tree area and the black dots are representing the point scatterers defined to a tree.

Since (2) and (3) are used to characterize the propagation behavior of the point scatterers, each tree is modeled using the specific set of input parameters α, β and Att_k, which will depend on the tree physical characteristics, e.g., size, leaf density, species, etc.

However, by successively applying the phase function for different values of α and β, it was observed that results converge for specific value sets. This allowed one to consider a simpler model, in which α was fixed at half-scale (0.5), while β was used to govern the tree re-radiation function.

C. Extraction Method of Final Tree Input Parameters for the Proposed Model

Modeling trees re-radiation function, using the proposed point scatterer formulation, requires the extraction of 2 input parameters from the measured re-radiation function of each particular tree. Therefore, the methodology followed in the extraction of β and Att_k parameters will be presented next.

To extract relevant tree parameters, the definition of a simulation geometry is required. Considering the flexibility in terms of shapes allowed by the model, the simulation geometry adopted in this study was set to be very similar to the one adopted for its practical validation. The transmitter was located at a distance of 1.15 m from the tree under simulation, while the receiver was rotated in an arc around the tree, at a constant radius of 0.7 m, from $\theta = -180°$ to $\theta = 180°$. In Fig. 6, the area defined as tree area as well as the 10 point scatterers assigned to the tree under simulation, are shown.

The input parameters were extracted after two different iterations. Firstly, both measured and simulated results were normalized to their maximum signal level. Assuming that Att_k parameter represents the insertion loss by the tree, by normalizing both signals to their maximum level, the influence of this parameter in the final result would be substantially minimized, allowing proper fine tuning of β. To this extent, several values of β were computed so that the ideal value was evaluated through a RMSE minimization process. In Fig. 7(a), 3 iterations of this process are depicted, for the β values of $10°$, $25°$ and $40°$.

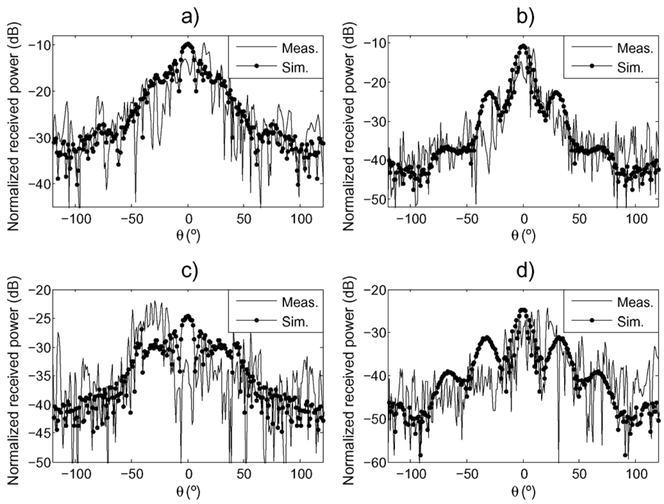

Fig. 8. Measured and predicted re-radiation function: *ficus* tree #1 at a) 20 GHz and b) 62.4 GHz; conifer tree at c) 20 GHz and d) 62.4 GHz.

Following β evaluation, both measured and simulated results were again normalized, but this time to the free space signal level. Such normalization will allow one to determine the appropriate insertion loss caused by the tree and, therefore, the proper evaluation of Att_k parameter. Again, this parameter is obtained using the same RMSE criteria. Three iterations of such optimization are shown in Fig. 7(b), for Att_k values of 10, 16 and 22 dB.

D. Results and Analysis

The proposed input parameter extraction method was applied to all 16 conifer and 13 *ficus benjamina* trees, at 20 and 62.4 GHz. Fig. 8 presents both measured and predicted re-radiation values for *ficus* tree #1 at 20 GHz (a) and at 62.4 GHz (b). It is important to observe that the results are normalized to the free space level. For this reason one may conclude that the presented model not only predicts, with a relatively good precision, the shape of tree re-radiation pattern, but also the correct signal level offset due to the insertion loss.

As per the conifer trees, the measured re-radiation patterns present relatively higher signal variability across the entire angular range when compared to the *ficus* trees. This is sought to be due to the higher foliage density and needle type leaves which, in turn enhances the diffuse scattering phenomena [2] emanated from the canopy, as shown in Fig. 8(c) and (d). Such phenomena becomes more pronounced at 62.4 GHz.

The proposed input parameter extraction method was then applied to all trees under study at both 20 and 62.4 GHz, so that β and Att_k parameters could be extracted. Tables I and II present results for *ficus* and conifer trees, respectively. The average RSME error between measured and predicted received signal levels across the entire angular range was observed to be consistently lower than 10 dB, despite some outliers as in the case of conifer trees. Overall, the model is capable of predicting, with relatively good accuracy, the 2D re-radiation patterns of isolated trees, for both species and frequencies, with RMSE average less than 8.1 dB.

TABLE I
EXTRACTED INPUT PARAMETERS FOR *ficus benjamina* TREES

	β (°)		Att_k (dB)		$RMSE$ (dB)	
Freq. Tree#	20 GHz	62.4 GHz	20 GHz	62.4 GHz	20 GHz	62.4 GHz
1	22,3	16,0	15,2	27,6	5,8	6,1
2	15,4	14,5	9,5	22,0	5,8	6,5
3	16,3	14,0	15,2	23,9	6,6	6,4
4	17,9	23,6	9,5	26,6	5,1	7,0
5	20,7	25,6	14,6	30,1	6,2	6,5
6	17,7	11,1	10,0	22,5	5,6	6,9
7	15,3	25,6	8,5	26,5	6,9	7,7
8	14,9	23,2	12,8	30,7	5,9	6,5
9	25,8	31,8	19,2	39,2	6,5	7,3
10	25,3	19,8	14,8	26,8	5,5	6,4
11	30,0	26,2	17,5	31,4	7,0	7,2
12	15,3	25,5	12,8	29,0	6,1	6,5
13	35,4	26,1	18,8	28,2	6,9	6,8
				Average	6,1	6,8

TABLE II
EXTRACTED INPUT PARAMETERS FOR CONIFER TREES

	β (°)		Att_k (dB)		$RMSE$ (dB)	
Freq. Tree#	20 GHz	62.4 GHz	20 GHz	62.4 GHz	20 GHz	62.4 GHz
1	34,9	30,5	29,9	41,8	7,3	7,4
2	39,7	23,8	22,5	34,5	6,6	8,2
3	44,3	34,3	23,8	40,4	7,2	6,8
4	40,9	52,2	25,5	45,7	7,4	6,5
5	53,9	33,3	26,0	38,0	6,8	8,0
6	74,0	29,0	25,4	35,6	7,5	10,4
7	40,7	38,5	23,9	40,5	6,5	8,7
8	34,3	49,7	22,5	44,7	7,9	6,2
9	34,9	32,7	23,2	38,3	6,2	7,3
10	22,8	25,7	18,4	33,8	6,0	7,3
11	34,0	42,5	20,1	40,7	7,0	7,2
12	34,9	35,7	21,6	37,8	8,2	9,2
13	42,1	38,1	24,7	42,2	8,2	8,4
14	70,3	61,0	26,5	44,4	6,7	7,5
15	39,0	27,1	24,5	35,6	6,3	7,8
16	41,3	33,1	26,7	42,5	9,0	12,1
				Average	7,2	8,1

V. PERFORMANCE ANALYSIS IN TREE FORMATION GEOMETRIES

Following the validation of the re-radiation pattern of several individual trees at 20 and 62.4 GHz, an extension of the proposed model to a tree formation will be presented. In this particular, interactions between several trees present in the formation will be considered, so that the proposed model can estimate the directional spectra at any position in the computation volume.

Based on the previous single tree characterization, simulations will be set to four different tree formation geometries, including some degree of inhomogeneity within the (computational) volume, as presented in the following subsections. Furthermore, the performance of the proposed model extended to tree formations, will be assessed, not only against dRET modeling approach [23], but also against measurement results obtained in a controlled environment, inside an anechoic chamber.

A. Methodology and Measurement Geometry

Four different geometries were used for validation purposes. These have been carefully defined in order to assess the model performance for both species and frequencies. To this extent,

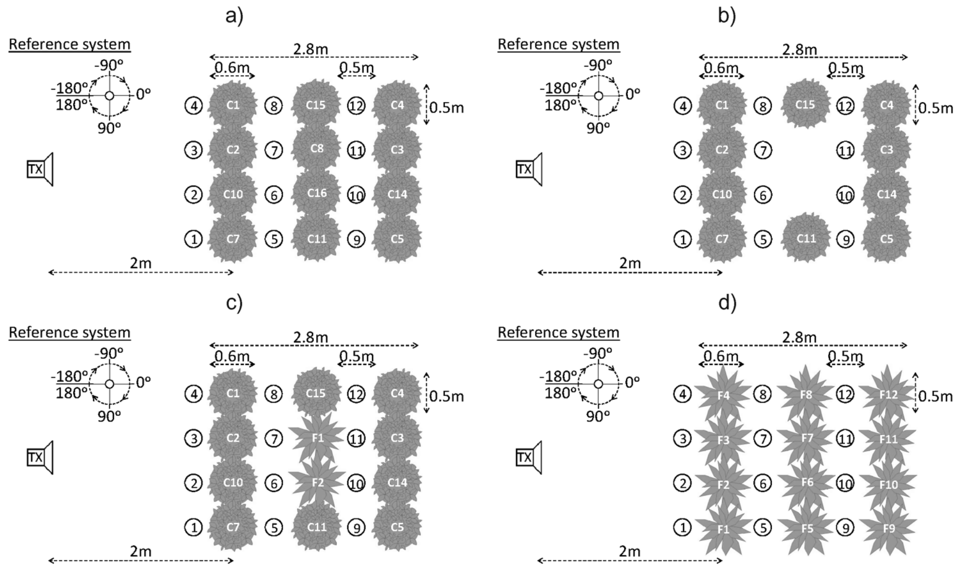

Fig. 9. Measurement geometries for tree formations: Tree formation a) #1; b) #2; c) #3; d) #4.

the same geometries were adopted for the proposed and dRET model assessments against measurement results.

Regarding the tree formation #1, depicted in Fig. 9(a), the transmitter was placed at a 2 m distance from the tree structure, composed by 12 conifer trees arranged in a 4×3 matrix, where the columns of trees were spaced out by 50 cm. The received signal was extracted with the receiver placed at one of 12 positions, represented by the white circles. At each receiver location, the receiving antenna was rotated around its vertical axis, in a $\pm 180^\circ$ range, with increments of 1°, recording the directional spectra in that position. As in re-radiation measurements, both transmitter and receiver were set to be at the same height, at 1.4 meters above the ground.

Tree formation #2, presented in Fig. 9(b), is similar to the previous one. However, in order to provide some inhomogeneity in the tree formation, conifer trees previously located at the center of the structure were removed. As previously, the receiver was placed at 12 different locations represented by the white circles.

In order to perform simulations combining the scattering effect of different tree species, the space between the conifer tree structure presented in formation #2, was occupied by 2 *ficus* trees, as in formation #3. This formation is illustrated in Fig. 9(c).

Finally, and to assess the performance of presented model while predicting the received signal inside a *ficus* tree formation, formation #1 was repeated, however, in formation #4, shown in Fig. 9(d), all trees were replaced by *ficus* trees. It is also important to mention that measurements were performed at 20 and 62.4 GHz, for all tree formations.

B. Proposed Model Simulation Geometries

Fig. 10(a) presents the geometry used in the simulations, where the transmitter was defined at 2 meters from the tree structure, composed by 12 trees positioned in a 4×3 matrix. Here, each tree is represented by 10 point scatterers. In each one of the receiver locations, the received signal was predicted in a $\pm 180^\circ$ angular range, with 1° increments.

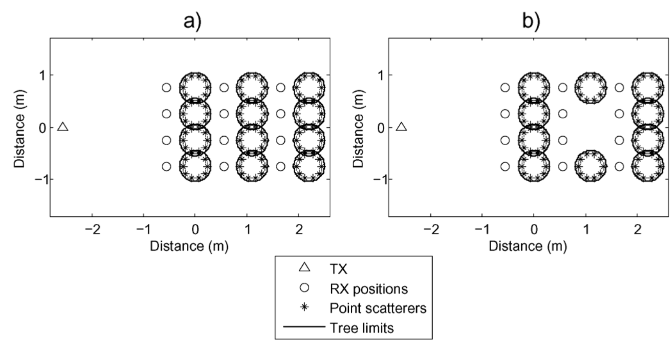

Fig. 10. Simulation geometry for tree formations: a) Formations #1, #3 and #4; b) Formation #2.

Assuming that the locations of the trees in all four geometries are the same, the simulation geometry presented in Fig. 10(a) was used to validate the model predictions against the measurement results obtained in formation #1, formation #3 and formation #4. In this case, only the tree input parameters were conveniently adjusted. As in formation #2, two trees were removed from the structure and therefore the simulation geometry had been adjusted to maintain coherence with the measurement geometry. The simulation geometry defined to assess results in formation #2 is depicted in Fig. 10(b).

C. dRET Simulation Geometries

Since the dRET model presented in [23] has been already proposed to model the propagation phenomena inside a tree formation environment, in addition to the practical validation, the dRET model was also used in the assessment of the proposed model. Hence, a comparative analysis against the dRET and measurement results will certainly strengthen the merit of the proposed propagation model.

For the purpose of the assessment against the dRET model, two different simulation geometries were defined. Regarding the geometry for simulations in formation #1, formation #3 and formation #4, the computational volume was divided in a 4×6

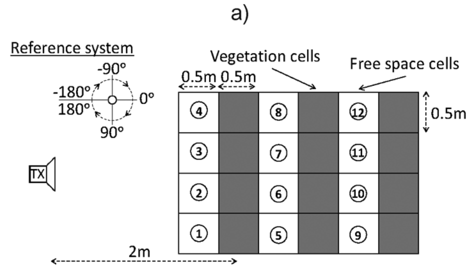

Fig. 11. dRET simulation geometry for tree formations: a) Formations #1, #3 and #4; b) Formation #2.

cell structure, as illustrated in Fig. 11(a), where the green cells represent the vegetation cells and the white cells represent the free space gaps, mimicking the spaces between trees. The numbered circles represent the locations where the received signal will be predicted by the model. The simulation geometry defined to mimic tree formation #2 is depicted in Fig. 11(b), where trees placed at the center of the tree structure were replaced by free space cells.

Beyond the definition of the dRET simulation geometries, it was also necessary to define the input parameters of the vegetation cells, such as the scatter function, the absorption coefficient (k_a), the extinction coefficient (k_e) and the scatter cross section (k_s) [22]. The definition of the scatter functions (or phase functions) was accomplished using one of the features of dRET, which allows the use of the actual measured re-radiation function, therefore reducing the error in the modeled scatter function. Despite the ongoing efforts in the extraction of the input parameters for foliage structures [1], [25] and given their implementation complexity, for the purpose of this paper, the parameters were obtained directly from [23].

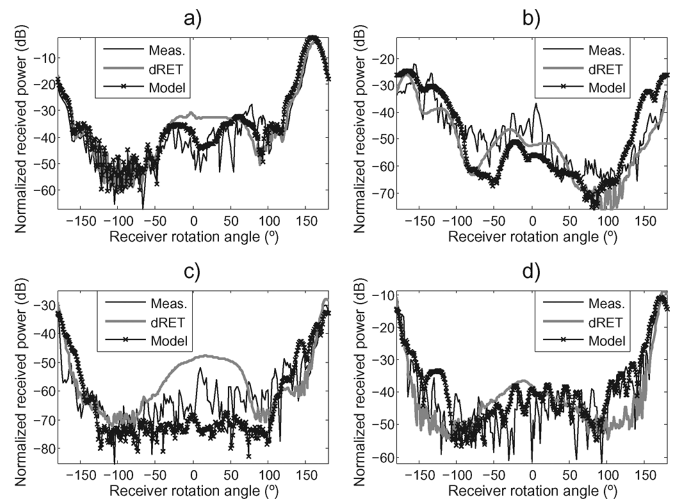

Fig. 12. Results for tree formations: a) formation #1 in position #4 and b) formation #2 in position #5, at 20 GHz; c) formation #3 in position #11 and d) formation #4 in position #7, at 62.4 GHz.

D. Measurement Results and Analysis

The proposed propagation model was used to predict the directional spectra at each one of the 12 receiver positions, for all tree formations, at 20 and 62.4 GHz. Simulation results were assessed not only against dRET model predictions but also against measurements performed in a controlled environment.

Results obtained from position #4 of the tree formation #1 at 20 GHz are depicted in Fig. 12(a). In this position, the received signal is highly influenced by the line-of-sight (LOS) contribution, and hence the directional spectra is mainly influenced by the receiver antenna radiation pattern. Similar behavior is expected and observed in positions #1 to #4 in all tree formations. Nevertheless, in -50° to 100° angular range, the receiver mainly receives the signal scattered by the tree structure and, as one may observe in Fig. 12(a), the proposed model yields a greater accuracy when compared to the dRET model, which overestimated the received signal in the angular range from -25° to 25°.

Fig. 12(b) presents results obtained from position #5 of tree formation #2. Unlike in LOS positions, in #5 the receiver is in a non line-of-sight (NLOS) situation, and thus, the received signal is now mostly influenced by the refracted (transmission) and scattered propagation modes. Results obtained from the proposed propagation model in the NLOS position #5, clearly indicate that such phenomena are modeled, since a relatively good agreement between predicted and measured results was achieved.

As the receiver is placed at larger vegetation depth inside the forest structure, namely at locations #9 to #12, it is more difficult to accurately estimate the received signal. This is due to the increase of the diffuse components caused by leaves and trunk scattering, and the reduction of the direct rays intensity due to foliage absorption. Notwithstanding, a rather relatively good accuracy is achieved by the presented ray-tracing simulation platform, when the receiver is placed behind the 3rd column of trees, clearly outperforming the dRET model in position #11 of tree formation #3. Results obtained in this position are depicted in Fig. 12(b).

As formation #4 is entirely composed by *ficus benjamina* trees, and as these present a sparser canopy when compared to conifer trees, both dRET and proposed models achieved a relatively good accuracy while predicting the received signal in NLOS situations. In Fig. 12(d), one may observe the results extracted from position #7 in tree formation #4 at 62.4 GHz, where both approaches presented similar performance while predicting the received signal directional spectra.

Subsequently, a quantitative assessment on the performance of both modeling approaches while predicting the directional spectra inside a tree formation was performed. For that purpose, the RMS error between the measured results and both the proposed and the dRET models were obtained for each of the 12 positions of all formations, at both 20 and 62.4 GHz. The RMSE values are depicted in Table III and Table IV, for proposed and dRET models, respectively. During this analysis, unexpected

TABLE III
RMS ERROR OBTAINED WITH PROPOSED MODEL

	RMS errors (dB)							
	Formation #1		Formation #2		Formation #3		Formation #4	
Freq. Pos.#	20 GHz	62.4 GHz	20 GHz	62.4 GHz	20 GHz	62.4 GHz	20 GHz	62.4 GHz
1	6,7	9,3	9,6	N/A	7,7	10,0	8,5	8,9
2	7,2	6,0	6,5	N/A	7,0	6,6	7,3	7,5
3	7,4	5,6	7,2	N/A	6,7	N/A	7,7	8,4
4	6,4	8,1	6,1	N/A	5,9	9,5	8,2	9,3
5	10,2	10,9	9,3	10,9	9,1	10,7	8,4	8,5
6	10,0	8,2	8,9	8,4	8,4	8,8	8,3	7,8
7	8,8	8,6	9,5	9,4	8,2	7,5	7,6	7,7
8	9,5	11,2	7,5	8,9	8,4	9,3	7,9	9,2
9	11,6	15,9	11,1	10,1	10,9	13,8	8,8	8,9
10	14,8	14,0	8,7	7,5	10,0	8,1	11,4	9,1
11	14,6	15,2	8,4	8,2	10,3	9,4	8,8	7,3
12	15,3	13,1	12,2	8,9	14,4	12,5	9,3	9,3
Mean	10,2	10,5	8,8	9,0	8,9	9,7	8,5	8,5

TABLE IV
RMS ERROR OBTAINED WITH dRET MODEL

	RMS errors (dB)							
	Formation #1		Formation #2		Formation #3		Formation #4	
Freq. Pos.#	20 GHz	62.4 GHz	20 GHz	62.4 GHz	20 GHz	62.4 GHz	20 GHz	62.4 GHz
1	5,8	7,6	7,6	N/A	7,0	8,5	7,8	7,7
2	6,6	5,7	5,9	N/A	6,6	6,4	6,7	7,0
3	7,1	6,0	5,8	N/A	6,2	N/A	6,6	7,1
4	8,0	6,6	7,0	N/A	7,0	8,0	6,6	7,9
5	6,9	9,4	7,3	7,5	7,2	8,2	11,0	7,6
6	7,1	8,7	8,1	8,9	8,5	8,3	8,2	7,3
7	9,7	9,3	9,8	9,5	8,5	9,6	7,8	8,1
8	8,3	8,7	8,8	8,0	7,9	7,6	7,6	8,5
9	8,5	10,7	6,8	9,7	8,4	10,2	11,6	6,6
10	11,9	10,1	9,0	10,3	9,8	10,2	12,3	10,2
11	12,3	9,7	11,4	11,7	11,2	9,8	13,0	9,1
12	9,6	8,3	9,6	9,7	10,6	9,0	12,8	8,4
Mean	8,5	8,4	8,1	9,4	8,2	8,7	9,3	8,0

errors were found on measurement results, therefore, a few not-available (N/A) values are presented. From these results, one may conclude that the dRET model presented a slightly better overall performance when compared with the proposed propagation model. Notwithstanding, given its simplicity and ease of integration with other planning tools, the performance achieved with the presented model is remarkably good since the RMSE was consistently below 15 dB. Table V presents a comparative analysis between the dRET and proposed models.

Finally, the work presented herein consists of an initial study on the feasibility of applying the ray-tracing to tree formations, so far based on simple knowledge of the actual measured re-radiation pattern of each individual tree. Nevertheless, should a better characterization and modeling of the individual tree radiation pattern be accomplished, then the overall model performance would undoubtedly lead to significantly better results. And thus, the proposed work opens up a new plethora of research ideas and challenges for the convergence of existing and future (commercial) radio planning tools.

TABLE V
COMPARATIVE ANALYSIS

Aspect	dRET model	Presented model
Accuracy	Relative good performance while predicting directional spectra inside tree formations;	Overall performance very comparable to dRET model;
Complexity	High complexity of implementation;	Reduced implementation complexity;
Input parameter extraction	Relatively high complexity in the evaluation of the 4 input parameters;	Relatively reduced complexity, only 2 input parameters are required;
Simulation time	Iterative model, needs to perform several iterations to reach stability;	A two-stage iterative model, does not need to stabilize;
Simulation flexibility	It requires the computation of the signal in the entire structure during a simulation;	Directional signal spectra can be obtained for one location only;
Geometry flexibility	Simulation geometries based on squared cell structures;	Continuous geometries allowing totally inhomogeneous formations;
Further enhancements	Availability to integrate different obstacles remains unknown;	Simulation channels can be addressed with ideal point scatterers, buildings and trees. May be extended to other obstacles.

VI. CONCLUSIONS

In this paper, a 2D proof-of-concept that extends the point scatterer formulation to vegetation areas was successfully presented. The performance of the propagation model in several tree formations, including inhomogeneous combinations of tree species, was evaluated and assessed, not only, against measurements performed at two spot frequencies, but also, against another specific modeling approach for vegetation, i.e., dRET model. From the obtained results, one can conclude that the accuracy of the presented model in a tree formation environment is relatively good given its simplicity and ease of integration into other ray-tracing planning tools. On the other hand, the model performance is comparable to that of the dRET model, in predicting the directional spectra inside a tree formation scenario. Furthermore, the proposed model can overcome the dRET limitation for large propagation distances.

Studies performed so far, suggested that point scatterer formulation applied to vegetation media may allow one to perform more complex simulations, considering, for instance, time-varying effects, due to either wind-induced dynamics or transmitter and/or receiver mobility. This may be accomplished by manipulating some input parameters (e.g., spatial and time distribution of the point scatterers).

A 3D extension to include trunk and ground layer effects and the interaction between layers is under consideration, as well as further assessment of the proposed model to other species and frequencies.

REFERENCES

[1] *Attenuation in Vegetation*, Recommendation ITU-R P.833-8, Radiocommunication Assembly, Sep. 2013.

[2] R. Caldeirinha, "Radio characterisation of single trees at micro- and millimetre wave frequencies," Ph.D. dissertation, University of Glamorgan, South Wales, U.K., Apr. 2001.

[3] N. Rogers, A. Seville, and J. Richter *et al.*, A generic model of 1–60 GHz radio propagation through vegetation—Final Rep. QINETIQ/KI/COM/CR020196/1.0, May 2002.

[4] M. Weissberger, An initial critical summary of models for predicting the attenuation of radio waves by trees Dept. Defense, Annapolis, USA, Tech. Rep. ESD-TR-81-101, 1982.

[5] COST 235, "Radio propagation effects on next-generation fixed-service terrestrial telecommunications systems," Luxembourg, 1995, Final Rep..
[6] M. Al-Nuaimi and R. Stephens, "Measurements and prediction model optimisation for signal attenuation in vegetation media at centimetre wave frequencies," *IEE Proc. Microw. Antennas Propag.*, vol. 145, pp. 201–206, Jun. 1988.
[7] Y. Meng, Y. Lee, and B. Ng, "Empirical near ground path loss modeling in a forest at VHF and UHF bands," *IEEE Trans. Antennas Propag.*, vol. 57, pp. 1461–1468, May 2009.
[8] A. Seville and K. Craig, "Semi-empirical model for millimeter wave vegetation attenuation rates," *Electron. Lett.*, vol. 31, pp. 1507–1508, Aug. 1995.
[9] A. Seville, "Vegetation attenuation modeling and measurements at millimetric frequencies," in *Proc. 10th Int. Conf. on Antennas and Propagation*, Edinburgh, U.K., Apr. 1997, vol. 2, pp. 5–8.
[10] F. Wang and K. Sarabandi, "A physics-based statistical model for wave propagation through foliage," *IEEE Trans. Antennas Propag.*, vol. 55, pp. 958–968, Mar. 2007.
[11] G. Cavalcante and A. Giarola, "Optimization of radio communications in media with three layers," *IEEE Trans. Antennas Propag.*, vol. 31, pp. 141–145, Jan. 1983.
[12] L. Li, T. Yeo, P. Kooi, and M. Leong, "Radio wave propagation along mixed paths through a four-layered model of rain forest: An analytic approach," *IEEE Trans. Antennas Propag.*, vol. 46, pp. 1098–1111, Jul. 1998.
[13] H. Israelsson and L. Ulander *et al.*, "A coherent scattering model to determine forest backscattering in the VHF-band," *IEEE Trans. Geosci. Remote Sensing*, vol. 38, pp. 238–248, Jan. 2000.
[14] S. Torrico, H. Bertoni, and R. Lang, "Modeling tree effects on path loss in a residential environment," *IEEE Trans. Antennas Propag.*, vol. 46, pp. 872–880, Jun. 1998.
[15] S. Torrico and H. Lang, "Wave attenuation prediction through a volume of random located lossy-dielectric branches—3-D vector transport theory," in *Proc. 6th Eur. Conf. on Antennas and Propagation (EUCAP)*, Prague, Mar. 2012, pp. 3342–3345.
[16] K. Chee, S. Torrico, and T. Kurner, "Radiowave propagation prediction in vegetated residential environments," *IEEE Trans. Veh. Technol.*, vol. 62, pp. 486–499, Feb. 2013.
[17] A. Lindenmayer, "Developmental algorithms for multicellular organisms: A survey of L-systems," *J. Theor. Biol.*, vol. 54, pp. 3–22, 1975.
[18] Y. Lin and K. Sarabandi, "A Monte Carlo coherent scattering model for forest canopies using fractal-generated trees," *IEEE Trans. Geosci. Remote Sensing*, vol. 37, pp. 440–451, Jan. 1999.
[19] F. Wang and K. Sarabandi, "An enhanced millimeter-wave foliage propagation model," *IEEE Trans. Antennas Propag.*, vol. 53, pp. 2138–2145, Jul. 2005.
[20] L. Foldy, "The multiple scattering of waves," *Phys. Rev.*, vol. 67, pp. 107–119, Feb. 1945.
[21] F. Wang, "Physics-based modeling of wave propagation for terrestrial and space communications," Ph.D. dissertation, Univ. of Michigan, , USA, 2006.
[22] R. Johnson and F. Schwering, A transport theory of millimeter wave propagation in woods and forest Tech. Rep. CECOM-TR-85-1, 1985.
[23] T. Fernandes, "A discrete RET model for micro- and millimetre wave propagation through vegetation," Ph.D. dissertation, University of Glamorgan, South Wales, U.K., 2007.
[24] T. Fernandes, R. Caldeirinha, M. Al-Nuaimi, and J. Richter, "A discrete RET model for millimeter-wave propagation in isolated tree formations," *IEICE Trans. Commun.*, vol. E88-B, pp. 2411–2418, Jun. 2005.
[25] S. Morgadinho, R. Caldeirinha, and M. Al-Nuaimi *et al.*, "Time-variant radio channel characterization and modelling of vegetation media at millimeter-wave frequency," *IEEE Trans. Antennas Propag.*, vol. 60, pp. 1557–1568, Mar. 2012.
[26] M. Didascalou and M. Younis, "Millimeter-wave scattering and penetration in isolated vegetation structures," *IEEE Trans. Geosci. Remote Sensing*, vol. 38, pp. 2106–2113, Sep. 2000.
[27] N. Goncalves and L. Correia, "A propagation model for urban microcellular systems at the UHF band," *IEEE Trans. Veh. Technol.*, vol. 49, pp. 1294–1302, Jul. 2000.
[28] F. Mani and C. Oestges, "A ray based method to evaluate scattering by vegetation elements," *IEEE Trans. Antennas Propag.*, vol. 60, pp. 4006–4009, Aug. 2012.
[29] C. Ho *et al.*, "Antenna effects on indoor obstructed wireless channels and a deterministic image-based wide-band propagation model for in-building personal communication systems," *Int. J. Wireless Inf. Netw.*, vol. 1, pp. 61–76, Jan. 1994.
[30] G. Durgin and N. R. T. Patwari, "An advanced 3D ray launching method for wireless propagation prediction," in *Proc. IEEE 47th Vehicular Technology Conf. (VTC)*, Phoenix, May 1997, vol. 2, pp. 785–789.
[31] N. Leonor, D. Ferreira, R. Caldeirinha, and T. Fernandes, "Ray tracing based model using point scatterers for time-Varying radio channels," in *Proc Conf. on Telecommunications - ConfTele*, Castelo Branco, Portugal, May 8–10, 2013.
[32] J. Jarvelainen and K. Haneda, "Sixty gigahertz indoor radio wave propagation prediction method based on full scattering model," *Radio Sci.*, vol. 49, pp. 293–305, Apr. 2014.
[33] F. Fontan and P. Espineira, *Modeling the Wireless Propagation Channel*, 1st ed. Hoboken, NJ, USA: Wiley, 2008.
[34] F. Ulaby, T. Haddock, and Y. Kuga, "Measurement and modeling of millimeter-wave scattering from tree foliage," *Radio Sci.*, vol. 25, pp. 193–203, May 1990.

Nuno R. Leonor was born in Leiria, Portugal, in 1988. He received the Licenciatura and Master of Science degrees in electrical and electronics engineering - telecommunications, from the School of Technology and Management, Polytechnic Institute of Leiria, Leiria, Portugal, in 2010 and 2012, respectively. He is currently working toward the Ph.D. degree at the University of Vigo, Spain, working on a generic doubly-selective 3D vegetation model using point scatterers.

Rafael F. S. Caldeirinha (M'00) was born in Leiria, Portugal, in 1974. He received the B.Eng. (Hons) degree in electronic and communication engineering and the Ph.D degree in radiowave propagation from the University of Glamorgan, South Wales, U.K., in 1997 and 2001, respectively. His research work focused on vegetation studies at frequencies from 1 to 62.4 GHz.

He is currently Head of the Antennas & Propagation (A&P-Lr) Research Group, Instituto de Telecomunicações, Leiria, Portugal, and a Coordinator Professor in mobile communications at the School of Technology and Management (ESTG), Polytechnic Institute of Leiria (IPL), Portugal. His research interests include studies of radiowave propagation through vegetation media, radio channel sounding and modeling and frequency selective surfaces, for applications at microwave and millimeter wave frequencies. He has authored or coauthored more than 80 papers in conferences and international journals, one book chapter, and four contributions to the ITU-R Study Group which formed the basis of the ITU-R P.833-5 (2005) recommendation.

Prof. Caldeirinha is a member of the editorial board of the *International Journal of Communication Systems* (IJCS), Program Chair of WINSYS International Conference between 2006 and 2012, Appointed Officer for Awards and Recognitions of the IEEE Portugal section since 2014, and a Member of IEEE and IET.

Telmo R. Fernandes (S'05–M'06) received the Licenciatura degree in electrical engineering, telecommunications and electronics and the M.Sc. degree from the Sciences and Technology Faculty, University of Coimbra, Portugal, in 1996 and 2000, respectively. His M.Sc. thesis was entitled "Channel Assignment on Cellular Networks using Neural Networks and Genetic Algorithms." He received the Ph.D. degree in radiocommunication systems from he University of Glamorgan, Glamorgan, South Wales, U.K., in 2007 for his research "Programme in Radiowave Propagation through Vegetation."

He is currently a Researcher at the Instituto de Telecomunicações, Leiria, Portugal. In 1997, he joined School of Technology and Management, Polytechnic Institute of Leiria, Leiria, where he is now a Senior Lecturer.

David Ferreira was born in Leiria, Portugal, in 1987. He received the Licenciatura and M.Sc. degrees in electrical and electronics engineering - telecommunications branch, from the School of Technology and Management, Polytechnic Institute of Leiria, Leiria, Portugal, in 2008 and 2010, respectively.

He is a Researcher at the Instituto de Telecomunicações, University of Coimbra, Coimbra, Portugal. He is currently working towards the Ph.D. degree in electrical engineering at the University of Vigo, Spain, and his current research interests include radio wave propagation measurements, characterization and modeling.

Manuel García Sánchez (S'88–M'93) received the Ingeniero de Telecomunicación degree from the Universidad de Santiago de Compostela, Spain, in 1990 and the Doctor Ingeniero de Telecomunicación (Ph.D.) degree from the Universidad de Vigo, Spain, in 1996.

His research interests include studies of indoor and outdoor radio channel sounding and modeling for narrow and wide-band applications at microwave and millimeter wave frequencies, point-to-multipoint radio links, mobile communications, UMTS, WLANs and DVB-T distribution networks.